General Disclaimer

One or more of the Following Statements may affect this Document

- This document has been reproduced from the best copy furnished by the organizational source. It is being released in the interest of making available as much information as possible.

- This document may contain data, which exceeds the sheet parameters. It was furnished in this condition by the organizational source and is the best copy available.

- This document may contain tone-on-tone or color graphs, charts and/or pictures, which have been reproduced in black and white.

- This document is paginated as submitted by the original source.

- Portions of this document are not fully legible due to the historical nature of some of the material. However, it is the best reproduction available from the original submission.

Search in Extreme Ultraviolet and Far Ultraviolet Astronomy

NASA Grant NGR-05-003-450

Semi-Annual Status Report

For the Period

December 1, 1984 - May 31, 1985

Prepared August 11, 1985

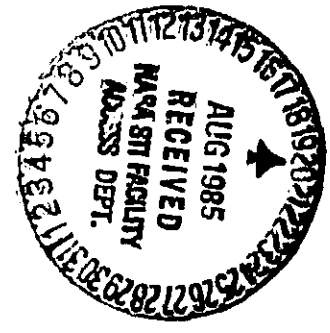

Prepared by:

Simon E. Labov

Simon Labov

Approved by:

for C. Stuart Bowyer

C. Stuart Bowyer

(NASA-CR-176068) RESEARCH IN EXTREME ULTRAVIOLET AND FAR ULTRAVIOLET ASTRONOMY Semiannual Status Report, 1 Dec. 1984 - 31 May 1985 (California Univ.) 34 p
HC A03/MF A01

N85-33060

CSCL 03A G3/89

Unclas
21929

RESEARCH IN EXTREME ULTRAVIOLET AND FAR ULTRAVIOLET ASTRONOMY

NASA Grant NGR-05-003-450

Professor C. S. Bowyer, Principal Investigator

SEMI-ANNUAL STATUS REPORT

December 1, 1984 - May 31, 1985

We are currently working on six instruments designed to explore six different aspects of the far and extreme ultraviolet cosmic radiation. With these capabilities we are observing every class of astronomical object and contributing to every branch of astronomy from cosmology to the local interstellar medium. As well as contributing to astronomy and astrophysics, we are also developing the latest technologies for our instrumentation. We continue working on the forefront of detector development, and we are now implementing some of our new concepts in spectrometer design.

Our projects are in all different stages of development. Some are just beginning their design phase, while others are under construction, awaiting a flight opportunity or in the midst of post flight data analysis. The Far Ultraviolet Imager (FUVI) was flown on the Aries sounding rocket flight 24.015 on November 27, 1983. Its unique large format 75mm detector mapped out the far ultraviolet background radiation with a resolution of only a few arc minutes. Analysis of this data will indicate to what extent the far ultraviolet background is extragalactic in origin, and a power spectrum of the spatial fluctuations will have direct consequences for galaxy evolution.

The UVX project consists of two independent far ultraviolet spectrometers, one built by our colleagues at Johns Hopkins University and the other built here at Berkeley. Both instruments

are mounted in GAS containers, and supported by a Goddard Avionics Package which is housed in a third GAS container. This package has been calibrated and integrated at the Goddard Space Flight Center, and is currently waiting for an opportunity to fly on one of the orbiters. With identical pointings for the two instruments, any discrepancies between the Berkeley results and the Johns Hopkins results should be easily understood. The Berkeley spectrometer operates between 600 and 1900Å with 10Å resolution. It utilizes a holographically ruled toroidal grating to maintain spatial resolution with low scattering. This makes it possible to remove the flux from stars that would otherwise confuse the measurements of the diffuse background.

Another project well underway is the Diffuse EUV Background Spectrometer. This unique spectrometer design is being built to measure the emission from the local interstellar medium. Previous measurements suggest that much of the gas within 50 or 100 parsecs of the sun is at temperatures over 100,000 °K, such gas would produce line emission detectable for the first time with this spectrometer. The mechanical structure of the instrument is nearly complete, and samples of the optics have undergone vibration testing and EUV reflectivity and scattering testing. The flight optics are undergoing fabrication and alignment will begin soon.

A design review was held for this instrument at Wallops Flight Facility in late June, and the experimenter's data package presented there is attached here as an appendix. The instrument is scheduled to fly on the Nike Black Brant sounding rocket flight 27.086 from White Sands in January, 1986.

The remaining projects are all in their design phases. We have been able to apply many of our new concepts in spectrometer design to explore many unanswered questions. A novel eschelle configuration will allow us to build a high resolution spectrometer to measure emission lines in the diffuse far ultraviolet background. This background spectrometer is being configured within the constraints of a hitchhiker payload. An instrument designed for either an advanced Aries class Spartan, or for the regular Spartan system will produce high efficiency soft X-ray spectra with variable line spaced or concentric groove gratings. Finally, we are designing a high resolution EUV/FUV spectrometer to use at the prime focus of a one meter mirror. This instrument, a col-

laboration with the Astronomical Institute of the University of Tubingen, West Germany, would fly as an advanced Aries class spartan payload.

Experimenters Data Package for 27.086 UG

Principal Investigator:	Stuart Bowyer
Project Scientist:	Simon Labov
Experiment Engineer:	Rick Raffanti
Experiment Technician:	John Bogard

Space Sciences Laboratory
University of California
Berkeley, Ca. 94720

Prepared: May 1985

Table of Contents

1. Description of Experiment

Scientific Objective

Diffuse radiation in the extreme ultraviolet (EUV) was first detected with a UC Berkeley wide field broadband photometer on a sounding rocket (Cash, Malina and Stern, 1976). Since then, additional broadband observations have confirmed this detection and have set upper limits for the radiation in longer wavelength bands (Stern and Bowyer, 1979; Paresce and Stern, 1981; Paresce and Bowyer, 1976; Sandel et al., 1979; Kimble, 1983). However, no spectral measurements have ever been carried out in the 80 to 600Å range.

Through the discovery of soft x-ray background radiation (Bowyer, Field and Mack, 1968) we have learned that much of the local interstellar medium is filled with hot tenuous gas. The soft x-ray flux indicates a gas temperature of 10^6K; most workers in this field agree that this gas is produced by supernova explosions.

Stern and Bowyer (1980) show that the EUV background does not originate from stars, but is consistent with emission from gas almost an order of magnitude cooler than the gas which produces soft x-rays. Absorption lines of OVI detected by the Copernicus satellite indicate that such gas does exist (Jenkins, 1978). The origin of this 10^5K gas is much more controversial. In the McKee and Ostriker (1977) model of the interstellar medium, this gas originates at the interface between the hot 10^6K gas and the cooler 10^4K clouds. In the "displacement" model of the local interstellar medium (McCammon et al., 1983) such interfaces would only exist on the outer edges of the "bubble" of 10^6K gas. A better knowledge of this 10^5K gas is crucial to advancing our understanding of the interstellar medium. In particular, spectral measurements of emission lines from the diffuse EUV radiation would confirm the thermal nature of this gas and indicate its temperature or distribution of temperatures; something that cannot be done with photometric measurements.

The Optical Design

A specialized instrument is required in order to perform observations of diffuse EUV emission. Sensitivity to diffuse radiation depends on solid angle and area, and therefore requires a fast optical system. To obtain high throughput at wavelengths below 500Å it is necessary to use grazing incidence optics. We have invented a novel spectrometer design incorporating grazing incidence optics and a large solid angle to produce spectra of moderate resolution from a diffuse source.

This spectrometer uses a wire grid collimator to restrict the field of view in one dimension to 40 arc minutes, while allowing 15° of sky to enter the instrument in the orthogonal direction. This wedge of light is then diffracted by an array of flat, reflection gratings at grazing incidence. The gratings are conventionally ruled with a blaze angle to maximize efficiency in this band. Once diffracted, the light is focused in the spectral direction by an array of mirrors, and passes through a thin filter to eliminate contamination from radiation at other wavelengths. The filter also seals the detector from particles or high pressure. The detector is a microchannel plate system with a wedge and strip type anode (Martin et al., 1981); a high yield photocathode is deposited on the front surface. The instrument's optical configuration is shown in Figure 1.

This instrument's mirrors are off-axis sections of parabolas of translation which would be difficult to construct by conventional means. We have developed a procedure to fabricate these mirrors that does not require the use of expensive diamond tooling machines or complicated polishing. We avoid the necessity of polishing by using float glass, which is naturally quite flat with low micro roughness. To form the curve in the glass we place it over a steel block with the desired form cut into the block's surface. The glass and block are then heated until the glass softens and

THE DIFFUSE EUV SPECTROMETER

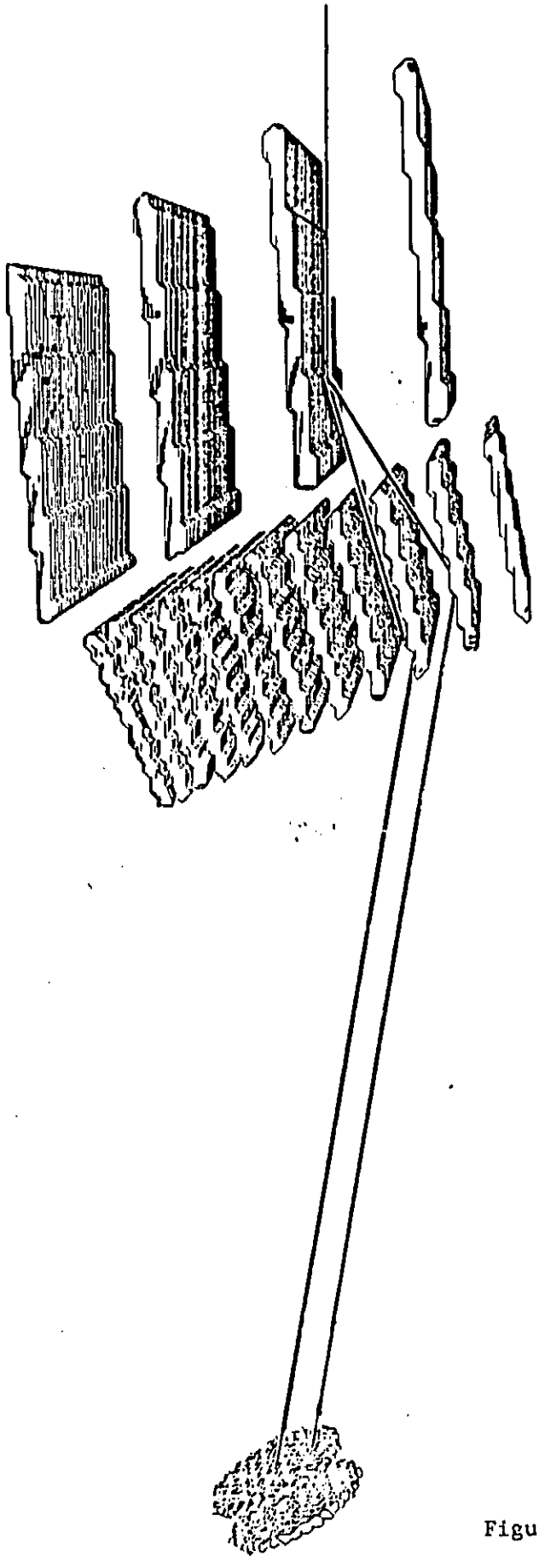

Figure 1.

sags onto the surface. Laboratory tests have shown that with proper control, the glass will maintain the correct shape and surface finish as the materials are cooled. A standard milling machine cannot cut an off axis section of a parabola into the block, but it can cut a section of an ellipse. By numerically matching sections of ellipses to the desired section of parabola we find that we can obtain a match which focuses quite well. Computer ray traces of the entire optical system show that these elliptical mirrors, with their expected errors in manufacturing, do not degrade the resolution of the spectrometer.

The general system described has many possible permutations and configurations. A large number of specific designs have been evaluated to find the optimum parameters for this novel spectrometer. The final design is comprised of three separate systems to cover wavelengths from 80Å to 650Å.

The resolution of the spectrometer was chosen to allow interesting sets of potentially strong lines to be separated from each other and from the much stronger airglow, geo-coronal and interplanetary lines that crowd the spectrum. Near 150Å the resolution (λ / $\Delta\lambda$) is 15; it rises to 50 at 584Å, preventing the bright HeI line from spreading over many interesting interstellar lines. The minimum detectable flux in a 350 second observation ranges from 80 to several hundred photons cm^{-2} sec^{-1} str^{-1}, providing far more sensitivity to a single line than previous photometric instruments. Figure 2 shows this instrument's resolution as a function of wavelength and Figure 3 shows its sensitivity to line radiation, along with the results of several broadband measurements.

Mechanical Design

The instrument has 67 optical elements that must be positioned within a few thousandths of an inch of their proper place. The design must allow for additional positioning flexibility to compensate for the errors inherent in the mirror fabrication process, and it must withstand the vibration of a space launch. Furthermore, baffles must be carefully placed to avoid "ghost" lines while blocking as little of the aperture as possible. We have developed an optical bench system that fulfills all of these criteria and has withstood vibration testing with glass elements in place. The design simplifies the alignment process by dividing the instrument into eight modules. Each module holds the glass parts with a small piece of softer material (Kel-F) that is captive in the larger module structure. Shims between the Kel-F and the module allow each grating or mirror element to be positioned independently. Once the modules' elements have been aligned with respect to each other, they are mounted to a larger support structure. The modules can then be aligned as eight simple units to provide the proper diffraction and focusing of light onto the detectors. The instrument's mechanical layout is presented in Figure 4.

References

Bowyer, S., Field, G., and Mack, J. 1968, Nature *217* , 32.

Cash, W., Malina, R., and Stern, R. 1976, Ap. J. (Letters) *204* , L7.

Jenkins, E.B. 1978, Ap.J. *219* , 845.

Kimble, Randy 1983, PhD. Thesis, "Observations of the EUV/FUV Radiation Fields," University of California, Berkeley.

Martin, C., Jelinsky, P., Lampton, M., Malina, R.F., and Anger, H.O. 1981, Rev. Sci. Instrum. *52* , 1067.

McCammon, D., Burrows, D.N., Sanders, W.T. and Kraushaar, W.L. 1983, Ap.J. *269* , 107.

McKee, C.F. and Ostriker, J.P. 1977, Ap.J. *218* , 148.

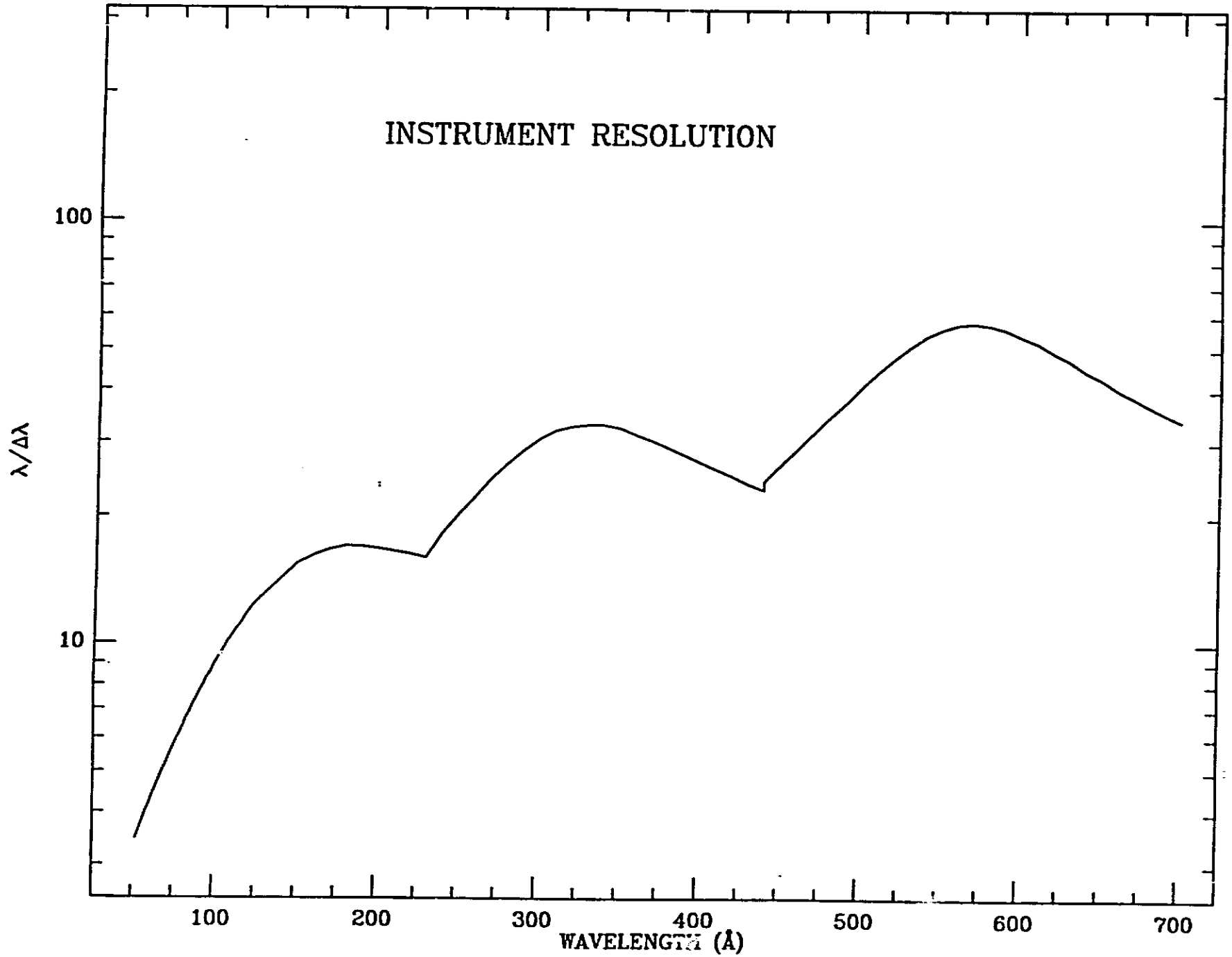

Figure 2.

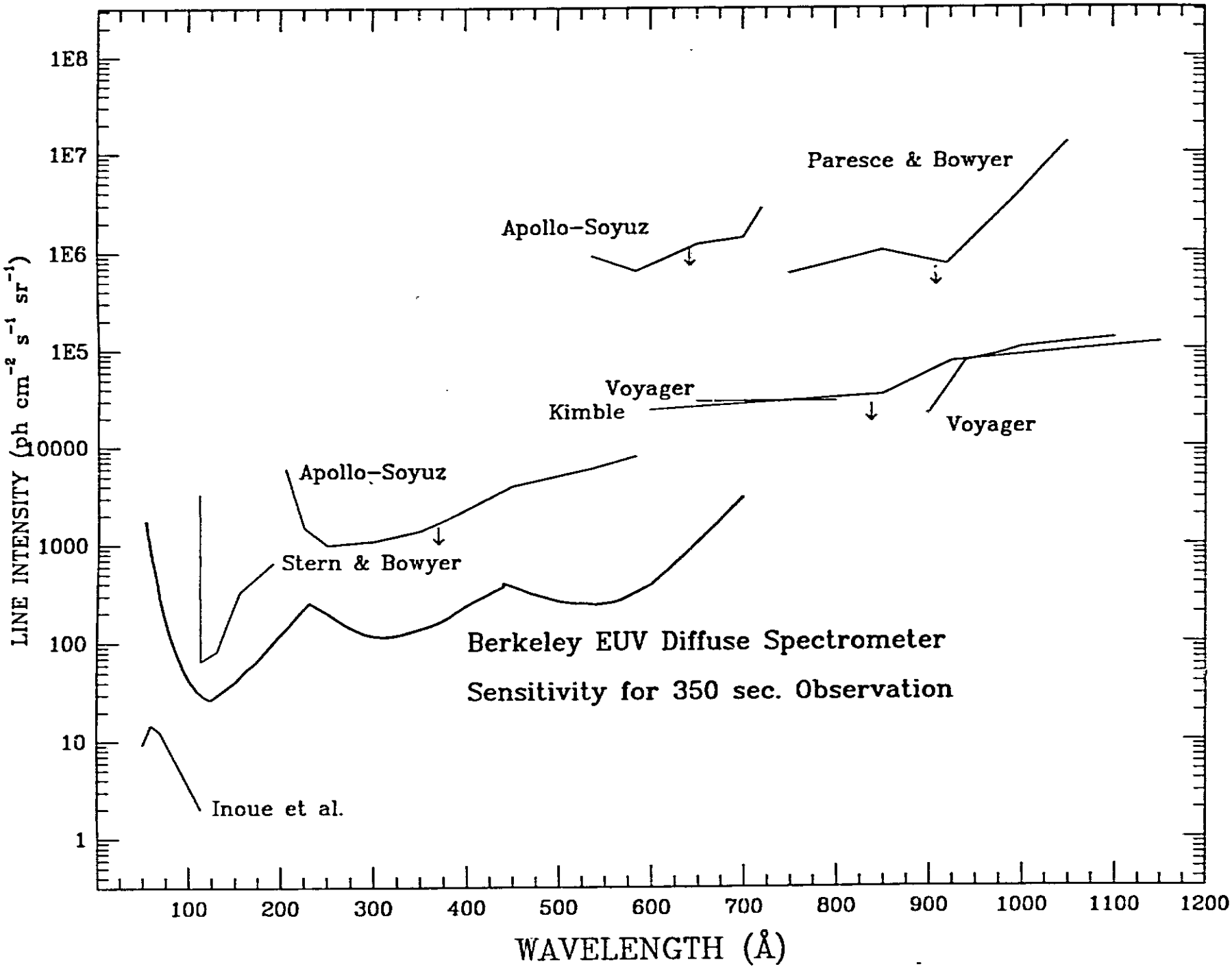
1E8
1E7
1E6
1E5
10000
1000
100
10
1
LINE INTENSITY (ph cm^{-2} s^{-1} sr^{-1})
Paresce & Bowyer
Apollo–Soyuz
Voyager
Kimble
Voyager
Apollo–Soyuz
Stern & Bowyer
Berkeley EUV Diffuse Spectrometer
Sensitivity for 350 sec. Observation
Inoue et al.
100
200
300
400
500
600
700
800
900
1000
1100
1200
WAVELENGTH (Å)

Figure 3.

THE DIFFUSE EUV SPECTROMETER

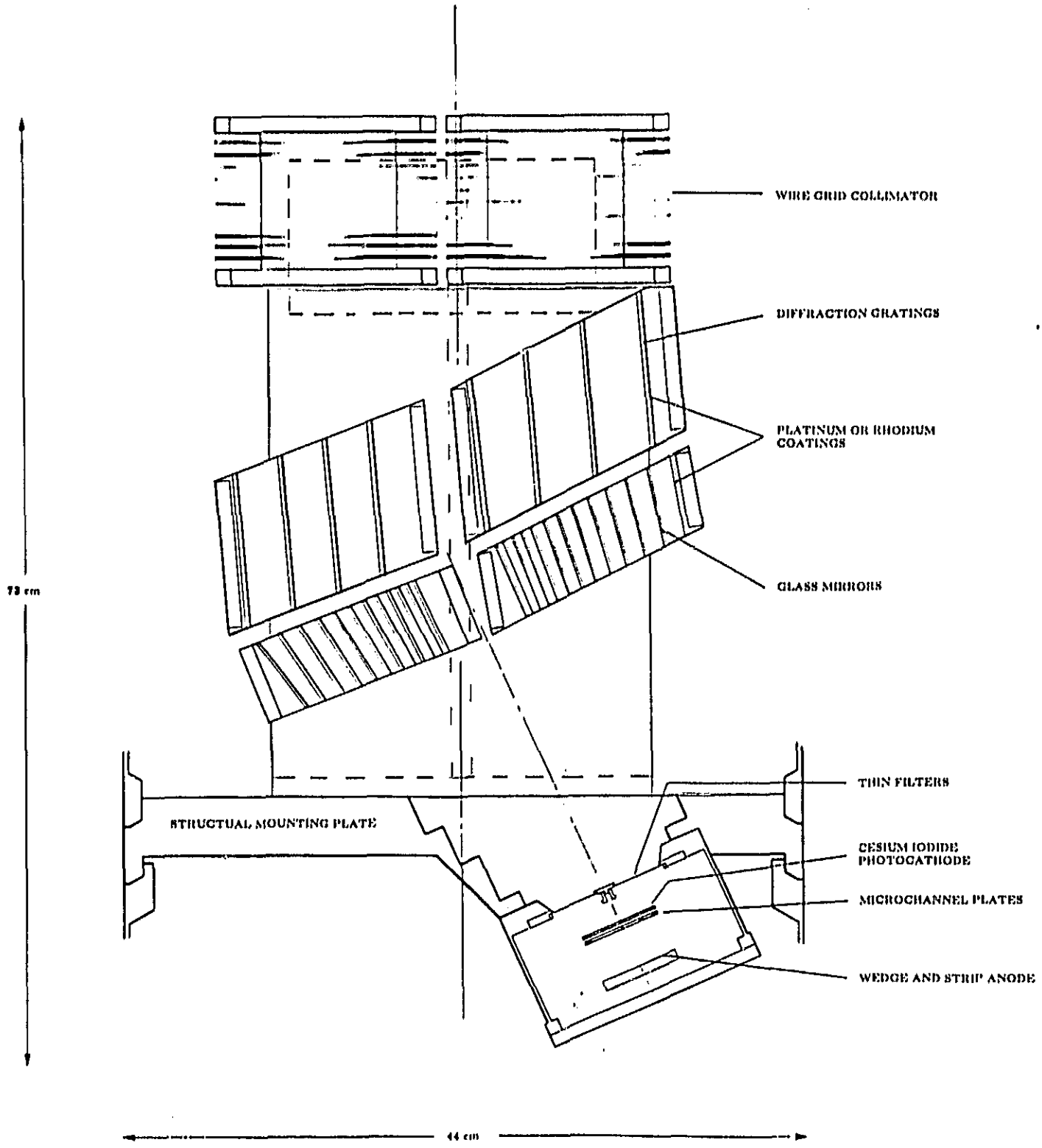

Figure 4.

Paresce, R. and Bowyer, S. 1976, Ap. J. *207*, 432.
Paresce, F. and Stern, R. 1981, Ap. J. *247*, 89.
Sandel, B. R., Shemansky, D. E., and Broadfoot, A. L. 1979, Ap. J. *227*, 808.
Stern, R. and Bowyer, S. 1979, Ap. J. *230*, 755.
Stern, R. and Bowyer, S. 1980, Astr. Ap. *89*, L1.

2. Block Diagram, Schematics, and Pin Lists

The block diagram is shown in figure 5. The schematics and pin lists are in Appendix A.

3. Experiment Configuration and Weights

The experiment has two sections. The forward section is a vacuum sealed cavity which houses the optics of the spectrometer. The aft section contains the electronics. The two sections are separated by the vacuum bulkhead which also forms the base of the spectrometer support structure. The detectors are in separate vacuum enclosures which can be isolated from the larger vacuum sealed optics cavity. The experiment parts are listed below along with their estimated weights and station locations.

EXPERIMENT SECTION	POUNDS	STATION	MOMENT
Tube 20°	1.5	79	118.5
Tube 6 in	2	79	158
Tube, Ion pump	1.2	78	93.6
Tube 90°	1.7	79	134.3
Bearings, grating	.2	67.1	13.42
Shims, grating	.06	67.1	4.026
Bearings, mirror	.02	71	1.42
Shims, mirror	.15	71	10.65
Washers, mirror	.29	71	20.59
Washer, active	.37	69	25.53
Ring, active	.28	69	19.32
Washer, plate	1.18	69	81.42
Screw, coll	1.59	61.3	97.467
Baffle, mirror	.6	71	42.6
Nut plate, coll	.21	61.3	12.873
Spacers, coll	5	61.3	306.5
Baffle, spec	.06	69	4.14
Filter cells	.06	78.2	4.692
Plate, grating	5.9	67.1	395.89
Side plate, grating	5.52	67.1	370.392
Plate, mirror	2.88	71	204.48
Side plate, mirror	2.56	71	181.76
Keeper plate, all	.3	69	20.7
T - special	1.36	84.7	115.192
Pump bracket	.33	78.5	25.905
Grid, collimator	5.28	61.3	323.66[illegible]
Claw, collimator	6.26	61.3	383.738
Sandwich plate, collimator	18.5	61.3	1135.35
Support plate, T, collimator	2.2	61.3	134.86

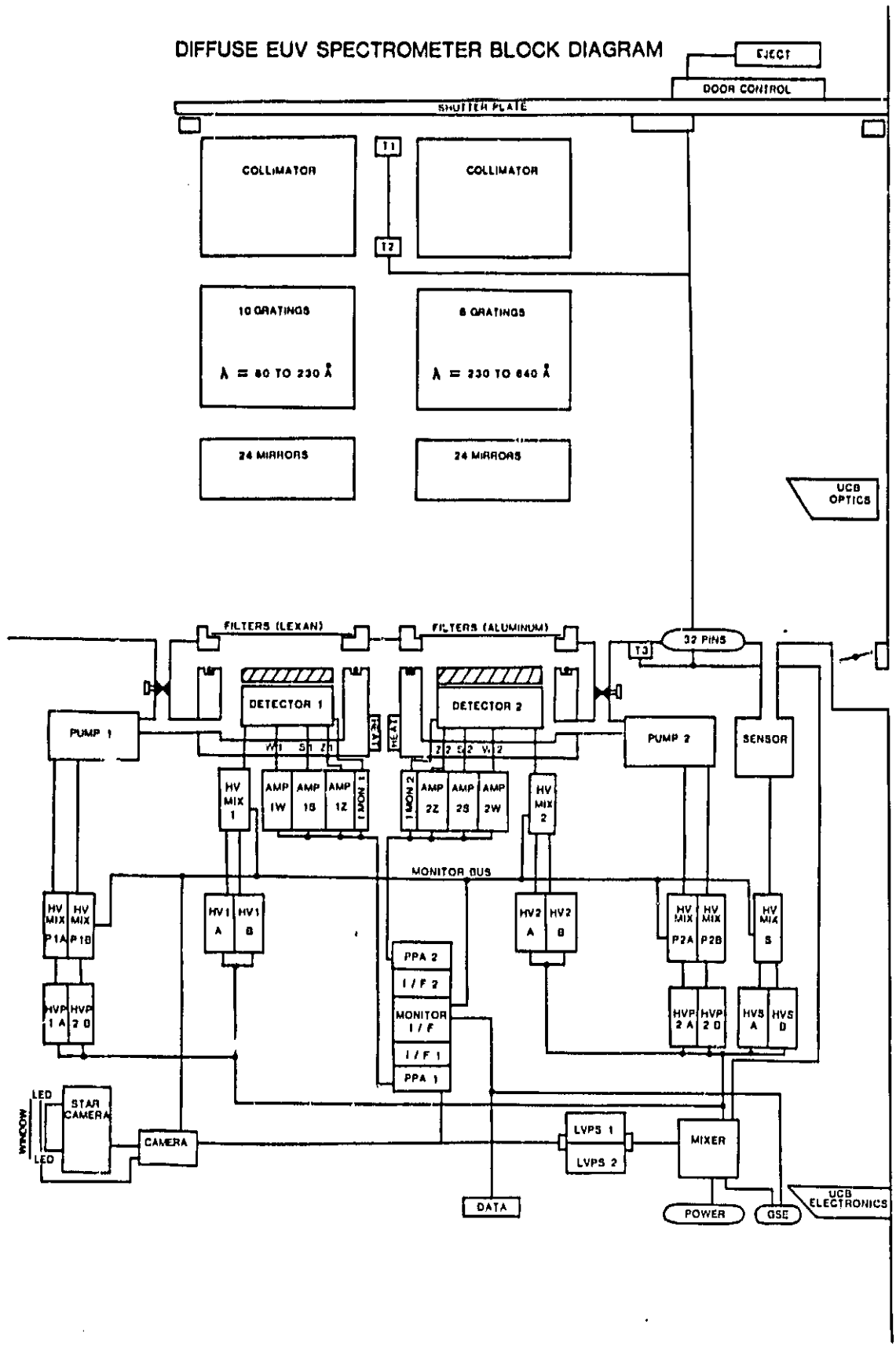
DIFFUSE EUV SPECTROMETER BLOCK DIAGRAM
EJECT
DOOR CONTROL
SHUTTER PLATE
COLLIMATOR
T1
T2
COLLIMATOR
10 GRATINGS
λ = 80 TO 230 Å
6 GRATINGS
λ = 230 TO 640 Å
24 MIRRORS
24 MIRRORS
UCB OPTICS
FILTERS (LEXAN)
FILTERS (ALUMINUM)
T3
32 PINS
DETECTOR 1
DETECTOR 2
PUMP 1
PUMP 2
SENSOR
HV MIX 1
AMP 1W
AMP 1S
AMP 1Z
1 MON 1
1 MON 2
AMP 2Z
AMP 2S
AMP 2W
HV MIX 2
MONITOR BUS
HV MIX P1A
HV MIX P1B
HV1 A
HV1 B
HV2 A
HV2 B
HV MIX P2A
HV MIX P2B
HV MIX S
HVP 1 A
HVP 1 B
HVP 2 A
HVP 2 B
HVS A
HVS B
PPA 2
I/F 2
MONITOR I/F
I/F 1
PPA 1
LED
STAR CAMERA
LED
WINDOW
CAMERA
LVPS 1
LVPS 2
MIXER
DATA
POWER
GSE
UCB ELECTRONICS

Figure 5.

Aperture plate, mirror	.44	70	30.8
T plate, base	1.32	76.4	100.848
Detector housings	6.5	80	520
Filter frames	.68	78.2	53.176
Bulkhead, modified	23	77.25	1776.75
Plate T	12	69.8	837.6
Plate T, support	2.45	67.8	166.11
Elbow, 4 inch	15	82	1230
Valve 4 inch	4.24	78.7	333.688
Pressure sensor	2.25	81.5	183.375
Ion pumps	30	82.4	2472
Valves, isolation	9	84.6	761.4
T. Manifold	2.61	82.8	216.108
Mirrors	2.74	71	194.54
Gratings	3.73	67.1	250.283
Detectors	16	79.8	1276.8
Collimator support plate	1.8	61.3	110.34
Detector back plate	3.43	81	277.83
Sensor supply	1.63	91.1	148.493
Ion pump supplys	7.26	98	711.48
Feedthru	.13	79.5	10.335
Electronics box	5	94.55	472.75
HV Bias	2.06	91.1	187.666
Mixers	1.75	91.1	159.425
Breakout box	2.06	92.8	191.168
LVPS	1.55	98.5	152.675
Imon and amps	2.75	82	225.5
Harnessing	7	94.5	661.5
LV support plate	6.3	94.55	595.665
HV support plate	8.9	97.3	865.97
LV support plate brackets	.95	94.55	89.8225
HV support plate brackets	1.3	97.3	126.49
Camera shelf	2.3	107.4	247.02
Camera	4.6	104.7	481.62
Camera brackets	2	104.7	209.4
Vacuum shell	50	67.28	3364
Electronics shell	70	93.9	6573
Shutter plate assembly	20	56.22	1124.4
Collimator mount	5.34	61.3	327.342
TOTAL EXPERIMENT	**408.63**		**32218.34**
Experiment center of Mass (station)			**78.8**

RECOVERY PAYLOAD

Experiment	408.63	78.8	32218.34
Parachute shell	40	148	5920
ACS without gas	105	131.5	13807.5
TM	56	116	6496

TOTAL RECOVERY PAYLOAD	**600.63**		**58441.84**
Recovery payload center of Mass (station)			**95.7**
Recovery payload center of Pressure			**105.5**

LAUNCH PAYLOAD

Experiment	408.63	78.8	32218.34
Parachute	75	148	11100
Parachute shell	40	148	5920
ACS with gas	110	131.5	14465
TM	56	116	6496
Fire and Despin	44	163.5	7194
Nose	35	34	1190
TOTAL LAUNCH PAYLOAD	**768.63**		**78583.34**
Launch payload center of Mass (station)			**102.23**

4. Experiment History

The payload is an entirely new type of spectrometer, and nothing like it has ever been built or flown in space. However, some of the subsystems of the instruments are similar or identical to those used on previous Berkeley experiments. About half of the electronics were flown on 24.015 and 24.004, and the other half are nearly identical to those flown previously. Flights 24.015, 24.004, 27.026 and 27.002 all had microchannel type detectors and vacuum ion pumps. We have used our experience from these flights to develop new and better detectors and pumps. The detectors and ion pumps in this instrument are prototypes for the Extreme Ultraviolet Explorer satellite project under development at Berkeley.

5. Times and Altitudes of Experiment Related Events

Function	Time	Altitude
Turbo pump removal	-15 min.	0 km
Filter check (from GSE)	-5 min.	0 km
Pump (1 and 2) power ON	+50 sec and ground command during flight	53 km
Pump (1 and 2) power OFF	+80 sec and ground command during flight	120 km
Sensor power ON	+50 sec	53 km
Sensor power OFF	+520 sec	77 km
Shutter plate OPEN	+70 sec	98 km
Shutter plate CLOSE	+500 sec	120 km
Experiment ON	+45 sec	41 km
Experiment OFF	+530 sec	53 km
Detector HV ON	+80 sec	120 km
Detector HV OFF	+520 sec	77 km

6. Pointing Requirements

The instrument will be despun, separated from the nose cone and booster, rolled so that the 45° VDA points north, and pointed in the target direction by T+90 seconds. This pointing will be in the anti-sun direction which is within 20° of the zenith in the winter. The pointing should remain steady to .25° and the absolute position should be within 3°.

At T+460 seconds a COW yaw maneuver will begin toward the southern horizon at 1°/second for 15 seconds and then continue in the same direction at the quickest rate possible (5 to 6°/second). When the zenith angle reaches 90°, the payload will hold until T+510 seconds.

7. Launch Window Requirements

The experiment is designed to measure the diffuse EUV background radiation which eminates from every direction in the sky. The objective in choosing a target direction is to minimize the non-interstellar "noise" radiation, and to maximize the interstellar signal.

The undesired "noise" radiation has three components all powered by the sun. When the sun shines on the earth, it dissassociates, ionizes and excites the atmosphere causing it to radiate. Not all the ions and atoms recombine and deexcite as soon as the sun goes down, this results in nightglow radiation. The strength of the EUV nightglow emission is not well known; existing measurements do not show any nightglow in the bandpass of interest. However, the sensitivity of this instrument is so great that nightglow levels far below previous detection limits would still interfere with the desired interstellar measurements. To minimize any such contamination, the observations should take place at midnight or later local time after most of the ions have recombined. To reduce the amount of atmosphere in the line of sight, the instrument should be pointed as close to the zenith as possible, and the observations made at the highest altitudes possible.

Contamination from nightglow can be monitored by several means. The contribution from the nightglow will change with altitude during the pointed portion of the flight. The scan to the horizon is done so that an even larger column of atmosphere can be observed, and by scanning to the south the observed atmosphere will all have had the same time in darkness. The portion of the sky within 60° of the zenith at White Sands is plotted in galactic coordinates in figure 6.

The second "noise" component comes from the geocorona. Ionized helium is trapped by the earth's magnetic field at distances up to several earth radii where they resonantly scatter the 304Å solar radiation. This contamination can be reduced by several orders of magnitude by looking along the earth's shadow. For typical geocoronal conditions, this shadow covers a circle in the sky with a radius of about 15°. The observations will therefore be made in the anti-sun direction.

The third source of contamination is from neutral helium in the earth's atmosphere and throughout the solar system; these atoms resonantly scatter solar radiation at 584Å. As the solar system moves through the galaxy, interstellar helium and hydrogen appear as a wind drifting past the sun. The sun gravitationally focuses the helium as it passes, causing a cone of higher density helium in the "down wind" direction. The strength of the 584Å emission depends on the helium density, therefore the observed strength varies with the time of year as well as the direction in the sky. Figure 7 shows the He 584Å line intensity as observed by the Mariner 10 UV Spectrometer. The data were collected on January 28, 1974 while the spacecraft was at a heliocentric distance of .757 AU. As shown in the figure the intensity only varies by a factor of two throughout the sky during that time of year. Figure 8 shows the ecliptic (which is where the sun's shadow travels) mapped in galactic coordinates. Plotted along the ecliptic are bars that show the 584Å intensity measured by the Prognoz 6 satellite in 1977. The measurements were made 15 times during 4 months, as the earth passed through the focussed cone of helium. The intensity peaks at about 10.5 Rayleighs near December 3 when the earth is directly down wind from the sun. By January 1, the intensity has dropped to 6.8 Rayleighs nearly as low as it was 4 months earlier far from the helium cone. The position directly down the helium cone is marked by the large triangle in figure

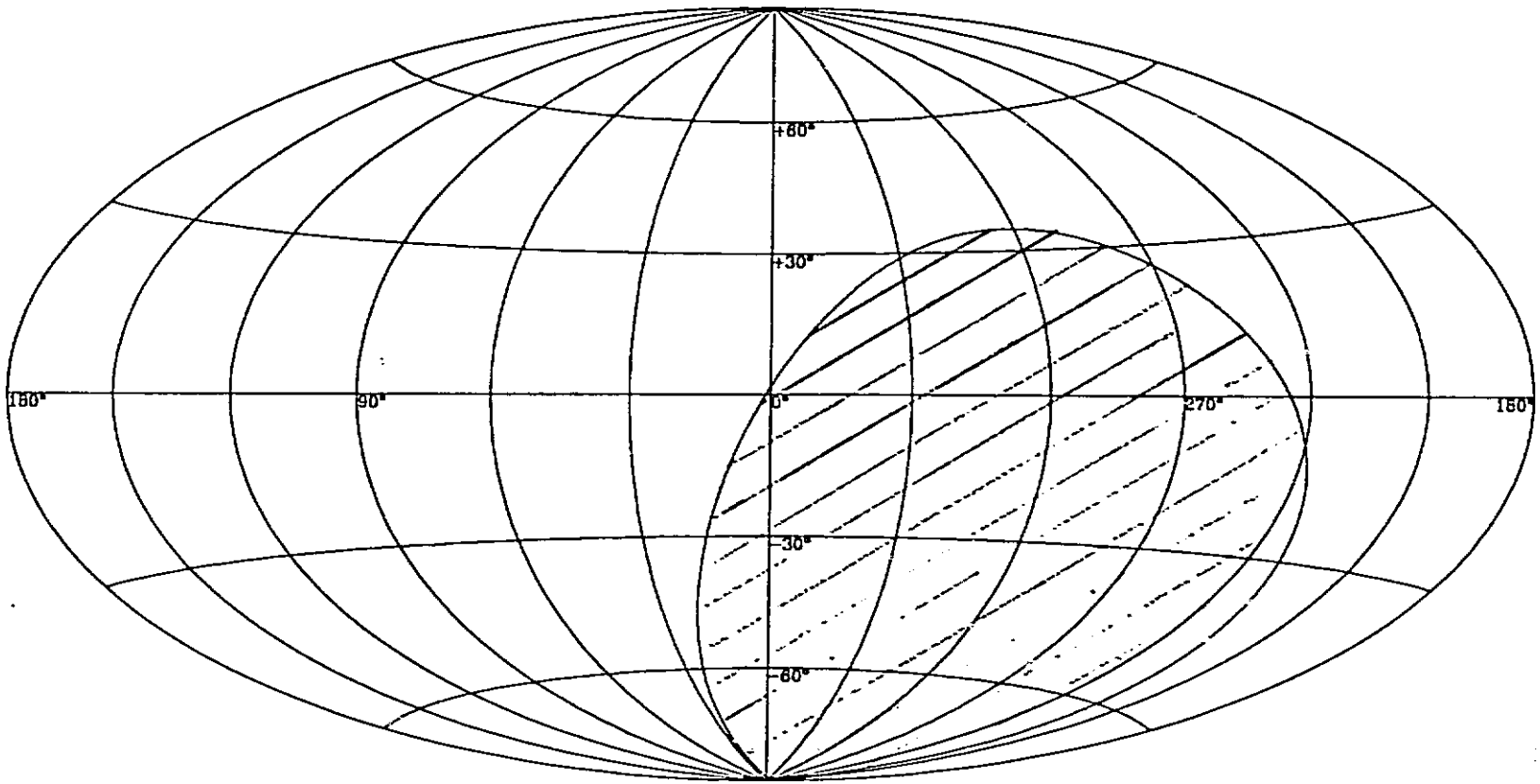

Figure 6. The hatched region is never observable within 60° of the zenith at White Sands. The map is in galactic coordinates.

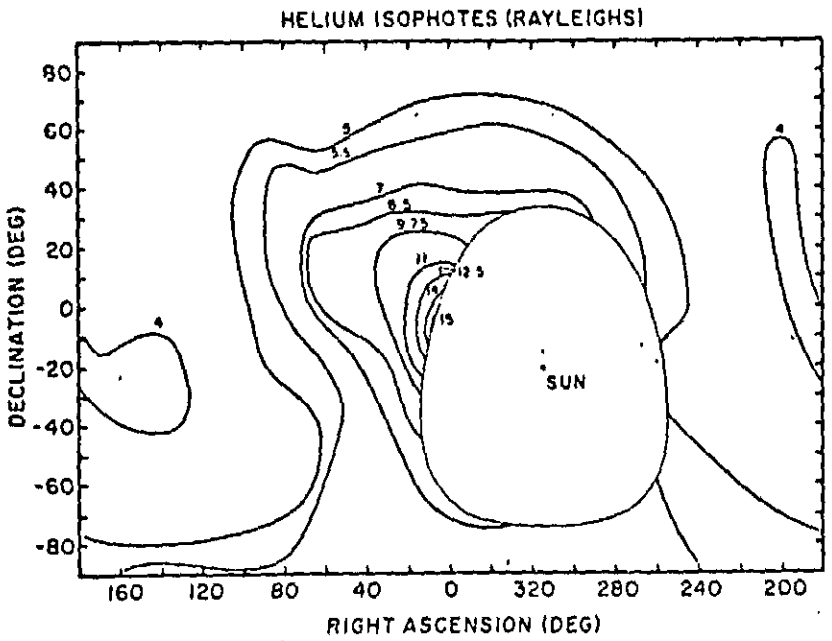

He 584 Å isophotes measured by the Mariner 10 UV Spectrometer

Figure 7.

8.

In summary, the opportunity to reduce HeII 304Å contamination is much greater than for reducing HeI 584Å contamination. Therefore we confine the observation to the anti-sun direction where the ionized helium is in the earth's shadow. Once confined in this way the 584Å intensity can be reduced slightly by not observing during November or December.

One final source of contamination for background measurements is point sources. Although this instrument is by far the most sensitive diffuse EUV spectrometer, its sensitivity to point sources is more moderate. Therefore only the brightest EUV point sources could contaminate the spectrum. Furthermore, the spectrum of an EUV star is so different from that of the interstellar medium that there is little danger of confusion. The only effect a bright EUV star would have on the observation would be to raise the "noise" level, thereby reducing the sensitivity. Since none of the seven known EUV stars are within 10° of the ecliptic, we need not be concerned with EUV point source contamination.

There are, however EUV sources in the sky that must be avoided. These are the planets and the moon. The moon moves across the sky so fast that it is only a potential problem for a few days near the full moon. In 1986 the moon is full on the following days: January 26, February 25, March 27, April 25, May 24, June 23, July 22, August 21, September 18, November 17, and December 16. None of the planets will be near the anti-sun direction during January or February 1986.

In addition to avoiding local "noise" radiation, the target direction should be chosen to maximize the desired signal. Previous observations of the diffuse EUV flux were made from a Berkeley sounding rocket, and from the Berkeley EUV photometers aboard the Apollo-Soyuz mission in 1975. The data is quite limited and the sky coverage is poor, but some trends are suggested by the map shown in figure 9. The pointed observations are shown by crosses, and the observed intensity is indicated by the size of the cross.

Any EUV emission from the interstellar medium is readily absorbed by interstellar hydrogen. Fortunately, the hydrogen is clumped, which leaves many lines of sight with little hydrogen to great distances. The hydrogen has been measured along the line of sight to many stars; 130 of them are plotted in figures 10, 11 and 12. Figure 10 shows the stars with an average density along the line of sight less than 0.05 cm^{-3}, figure 11 includes average densities from 0.05 to 0.5 cm^{-3}, and figure 12 includes densities above 0.5 cm^{-3}. The crosses on these figures indicate the log of the distance to the star. To maximize the EUV flux, we want to look in a direction where distant stars showed low average hydrogen density (n_H). Contours of column density vs distance from the sun have been derived from this data, and are shown projected onto the plane of the galaxy in figure 13. Notice that a low density region is suggested between 200° and 270° longitude.

Another way to indicate which directions have the least hydrogen is to look at interstellar reddening. This measures the interstellar dust, and the dust is usually associated with neutral hydrogen. Plots of reddening measurements are shown in figures 14, 15 and 16. Dust can also be observed by how it polarizes starlight. A map of these observations is shown in figure 17. All these dust measurements seem to confirm the existence of a "void" of material in between 200° and 270° galactic longitude.

To conclude, the best direction for the observations is in the anti-sun direction, after January 1, near the zenith, at local midnight, and between 200° and 270° galactic longitude. This restricts the flight to a launch window between January 15 and March 15, excluding January 25, 26, 27, February 24, 25 and 26 to avoid the moon.

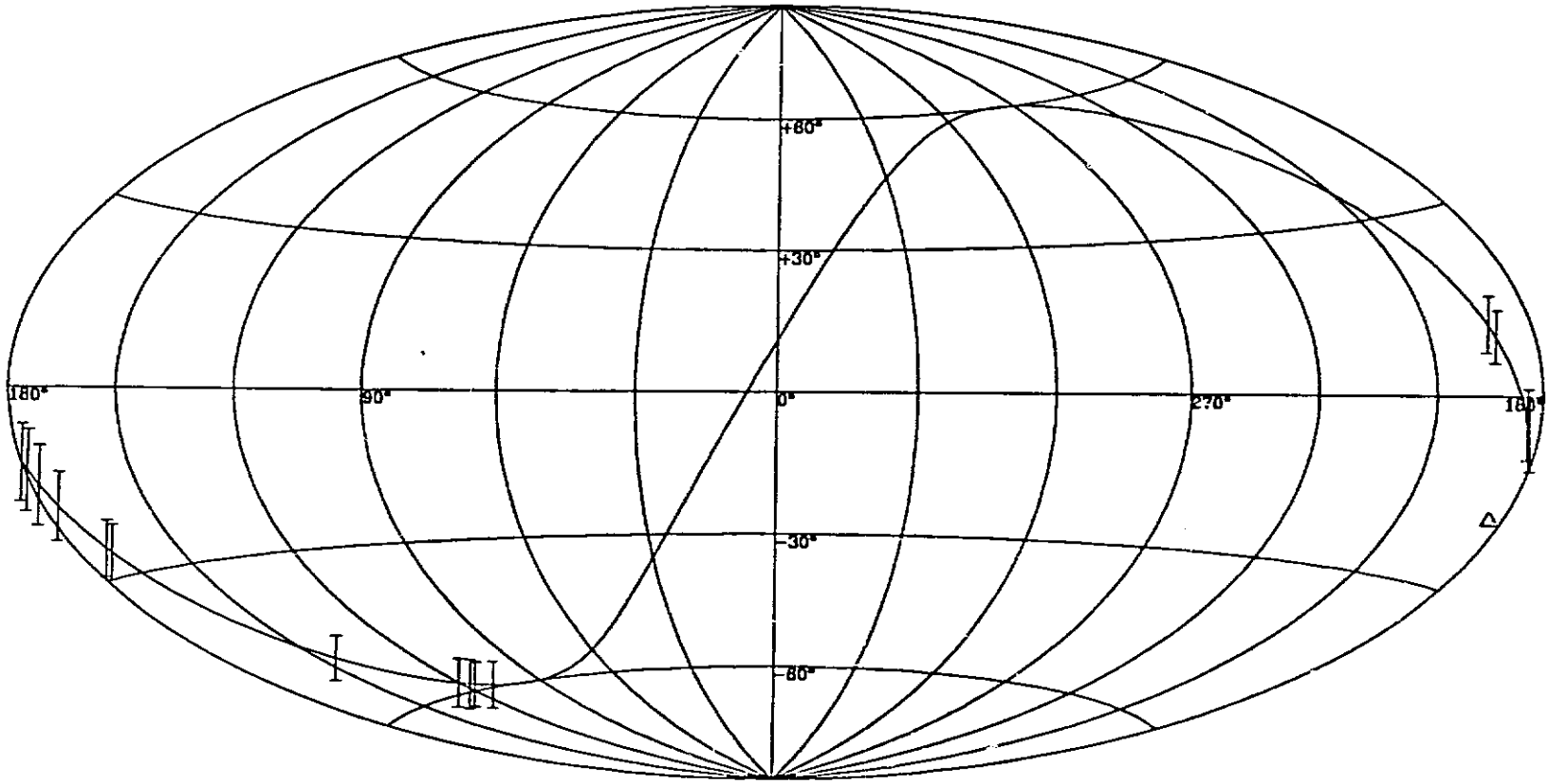

△ — indicates down wind He direction.

Figure 8. 584Å Antisolar direction

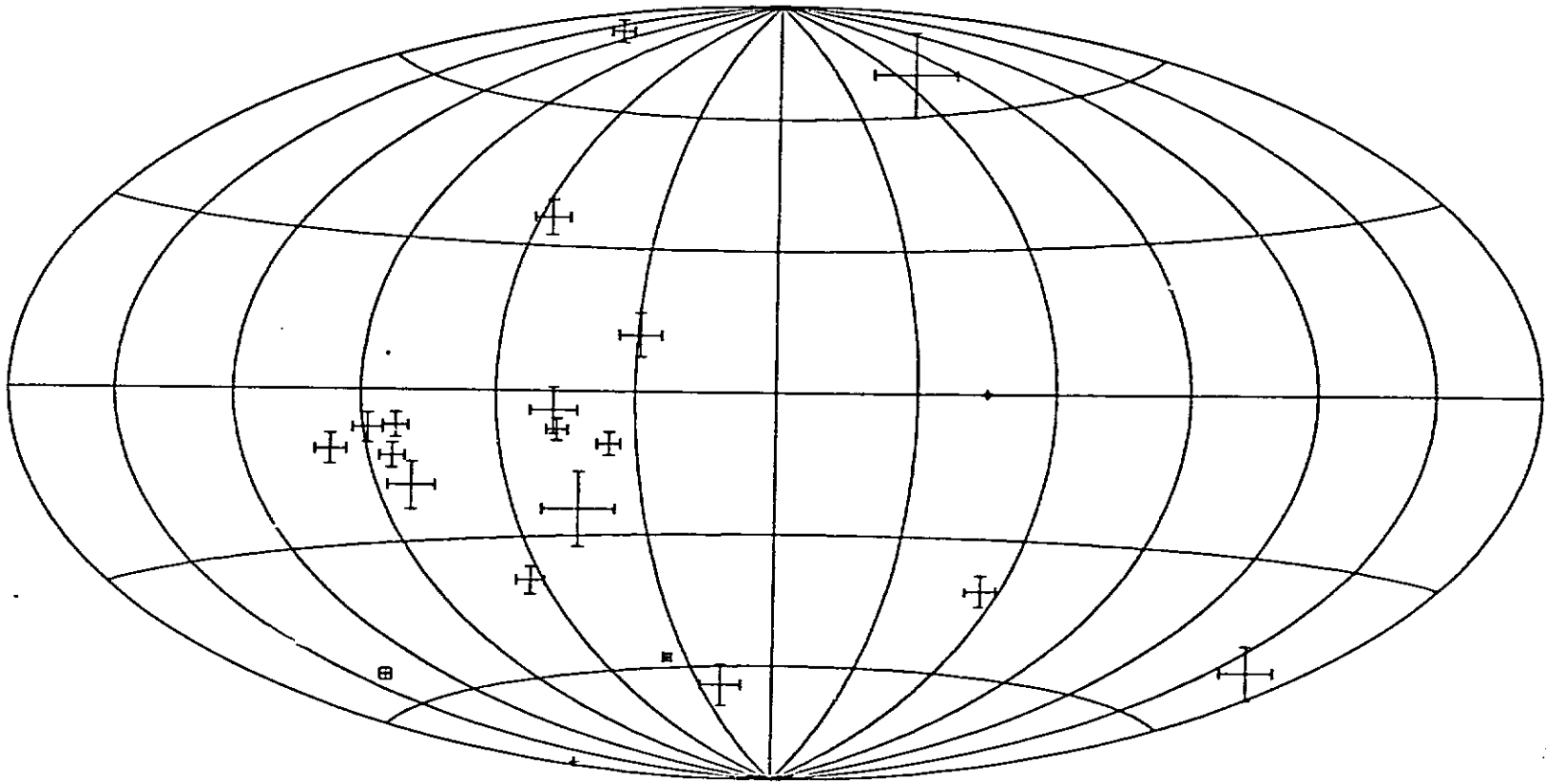

Figure 9. ASTP Par/Be countrates

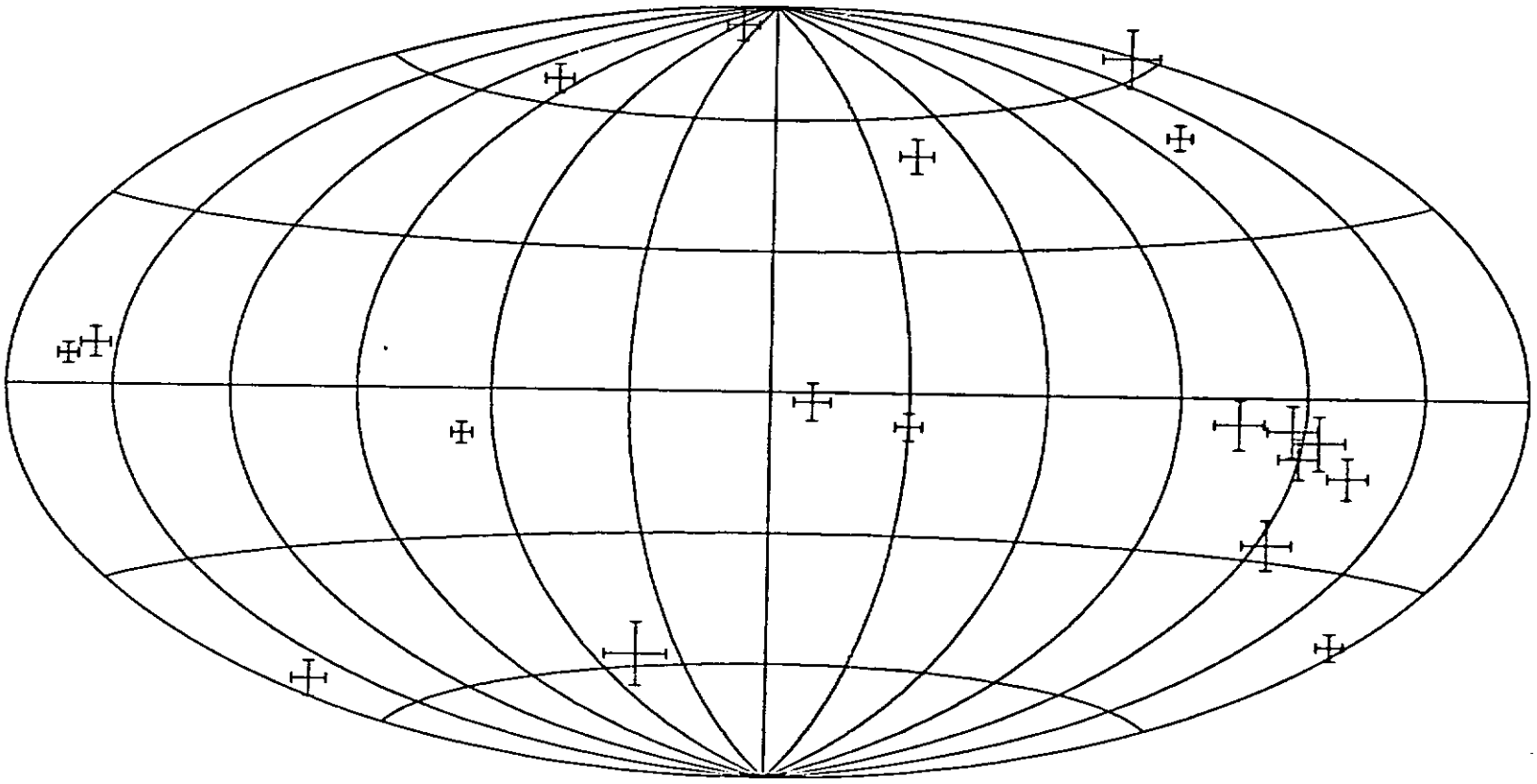

Figure 10. $n(H) < 0.05\ cm^{-3}$

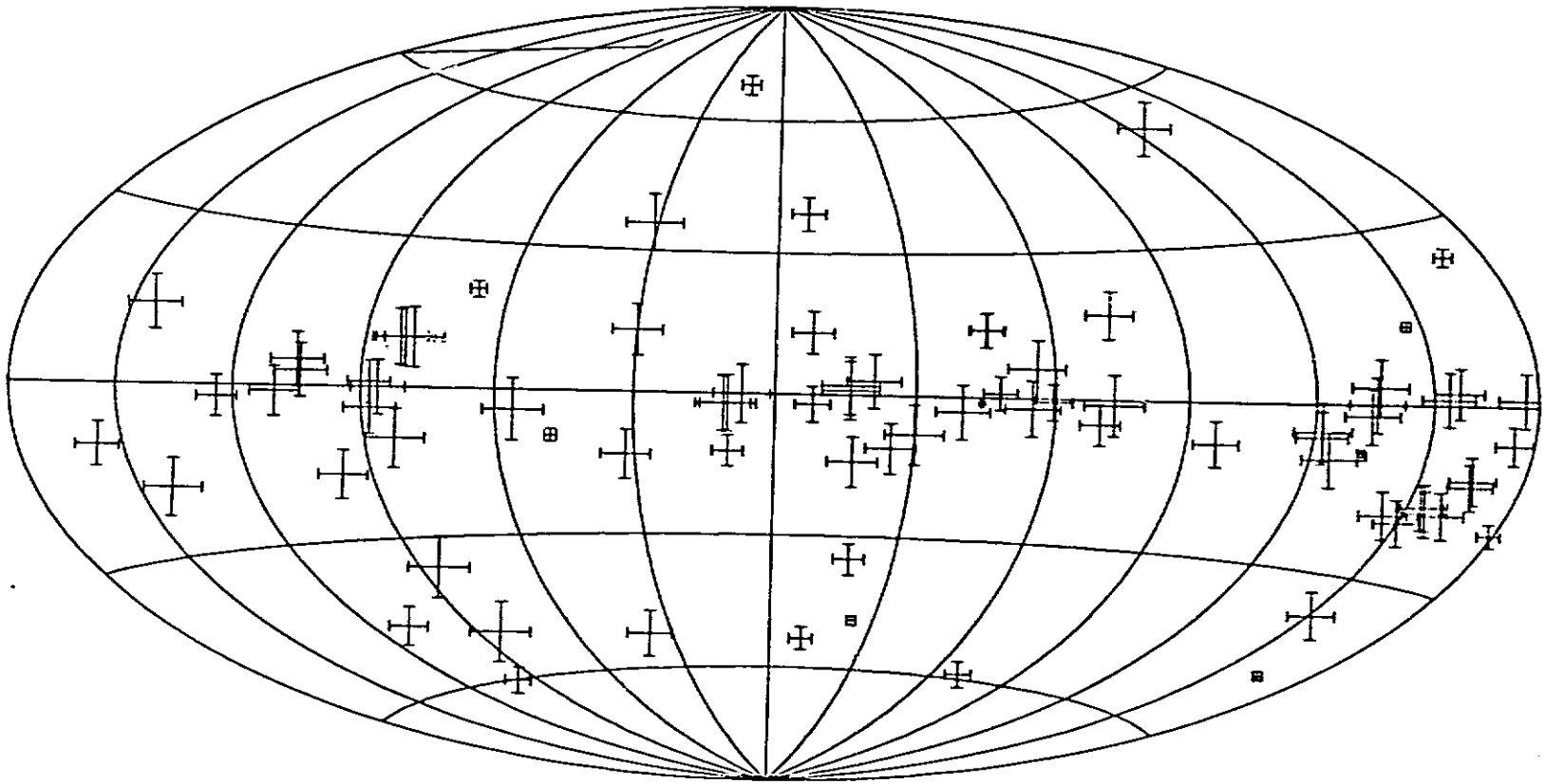

Figure 11. $0.05 < n(H)\ cm^{-3} < 0.5$

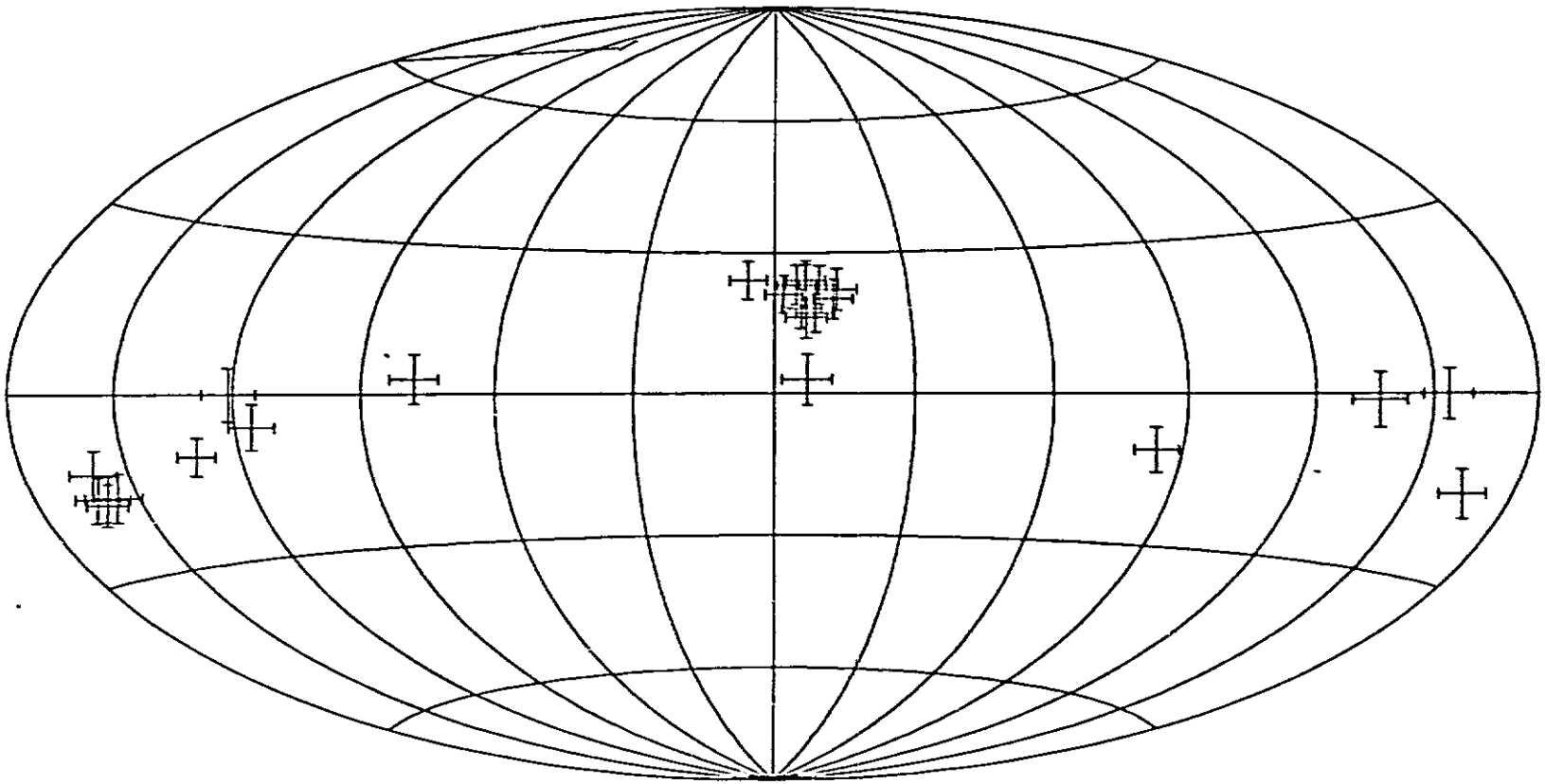

Figure 12. $0.5 < n(H)\ cm^{-3}$

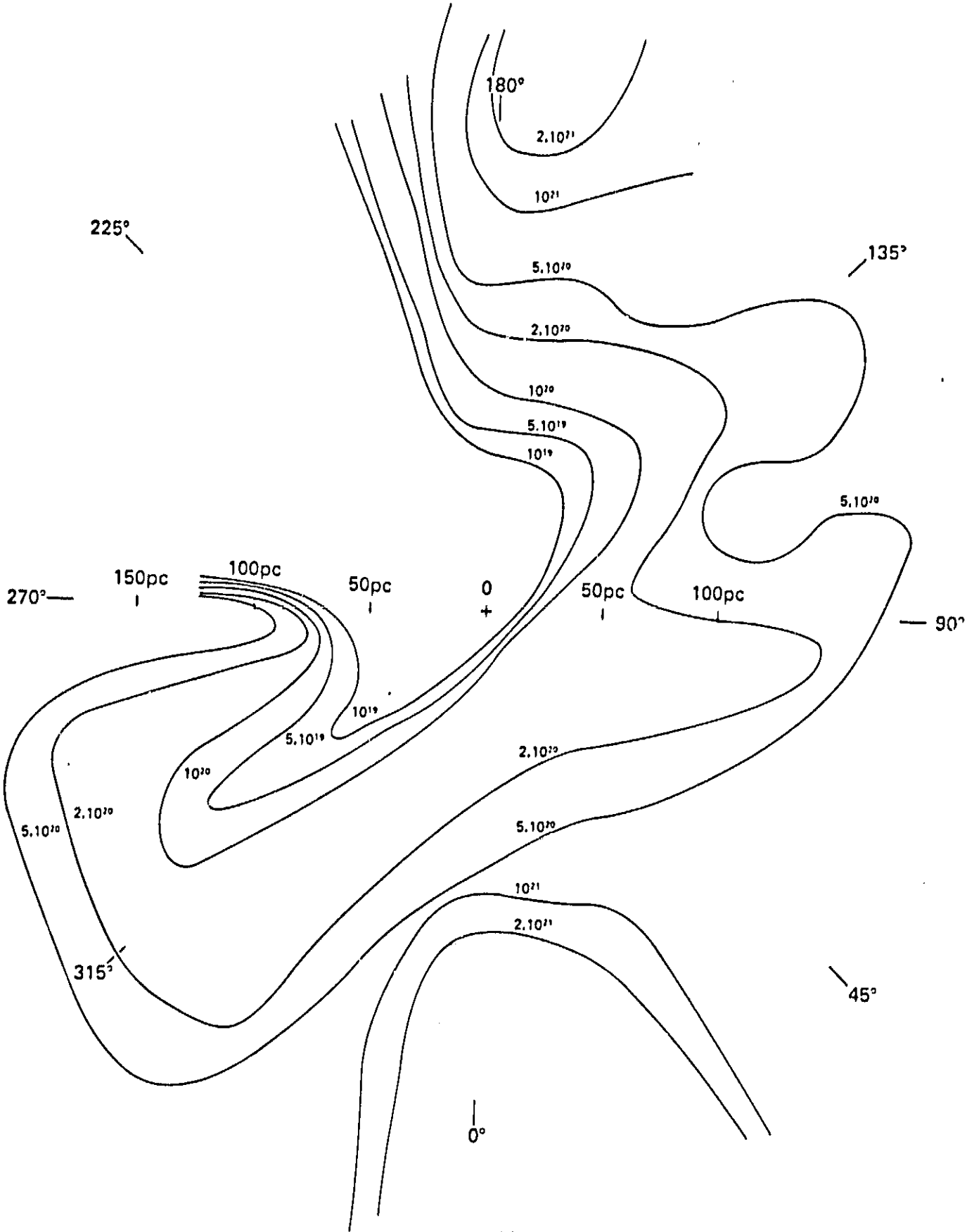
180°
2.10²¹
10²¹
225°
135°
5.10²⁰
2.10²⁰
10²⁰
5.10¹⁹
10¹⁹
5.10²⁰
270°
150pc
100pc
50pc
0
50pc
100pc
90°
10¹⁹
5.10¹⁹
2.10²⁰
10²⁰
5.10²⁰
2.10²⁰
5.10²⁰
10²¹
2.10²¹
315°
45°
0°

Figure 13.

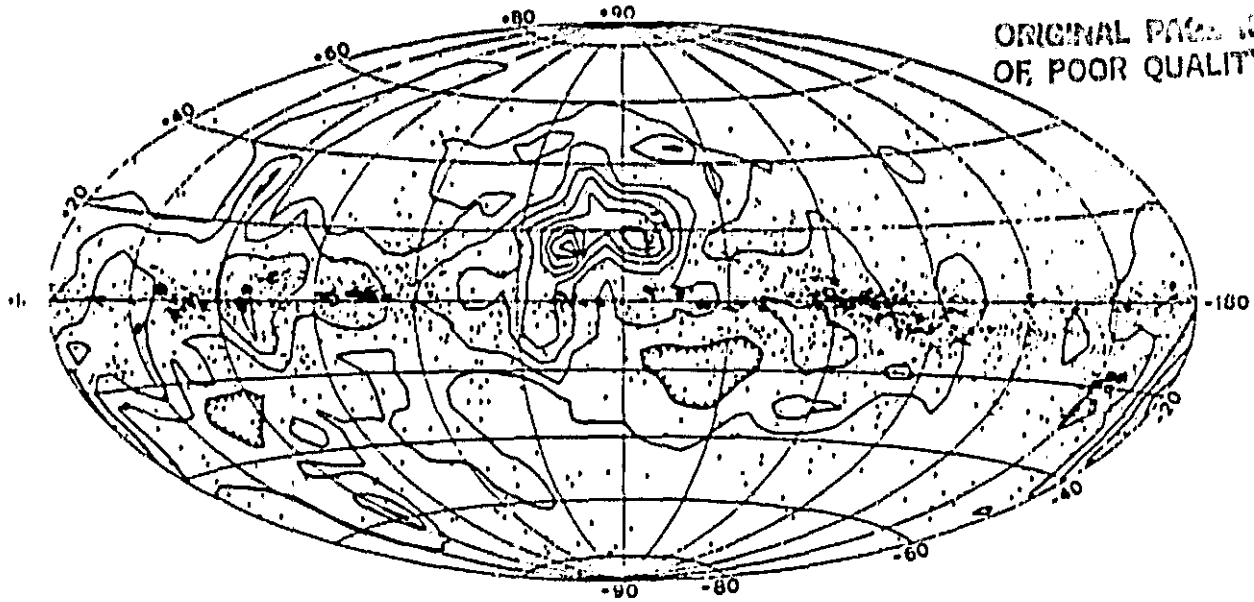

Aitoff equal area projection of the mean $E(B-V)$ per kiloparsec for OB stars within 2 kpc of the Sun. The center of the di ram is toward the Galactic center with longitude increasing to the left. Longitude lines are drawn every 30° and the parallels of la ude are drawn every 20°. The contour interval is 0.2 mag/kpc and the outermost contour is the lowest level. Contours surrounding de essed regions are indicated by tick marks

Figure 14.

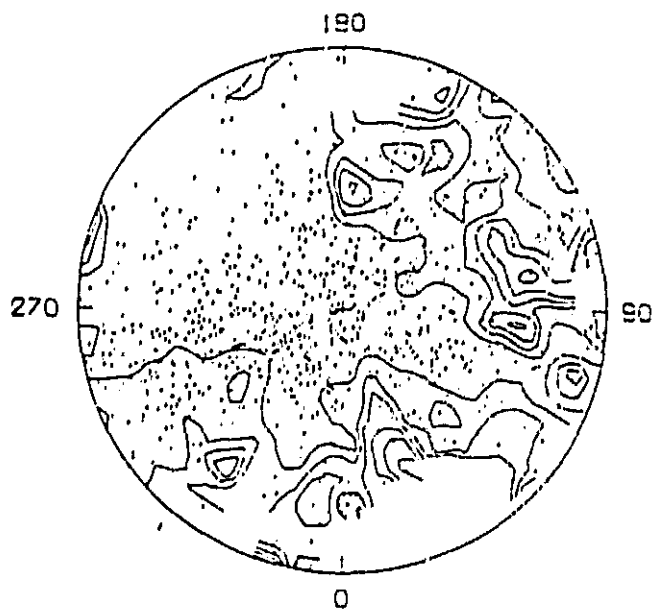

Color excess distribution in the Galactic plane out to 500 pc. The points indicate the positions of the OB stars used in the calculation. The contour interval is 0.1 in $E(B-V)$ generally increasing outward from the Sun. Depressions are indicated by tick marks on the contours. Only stars within 50 pc of the plane are used and the mean excesses were calculated using stars within 50 pc of a grid point

Figure 15.

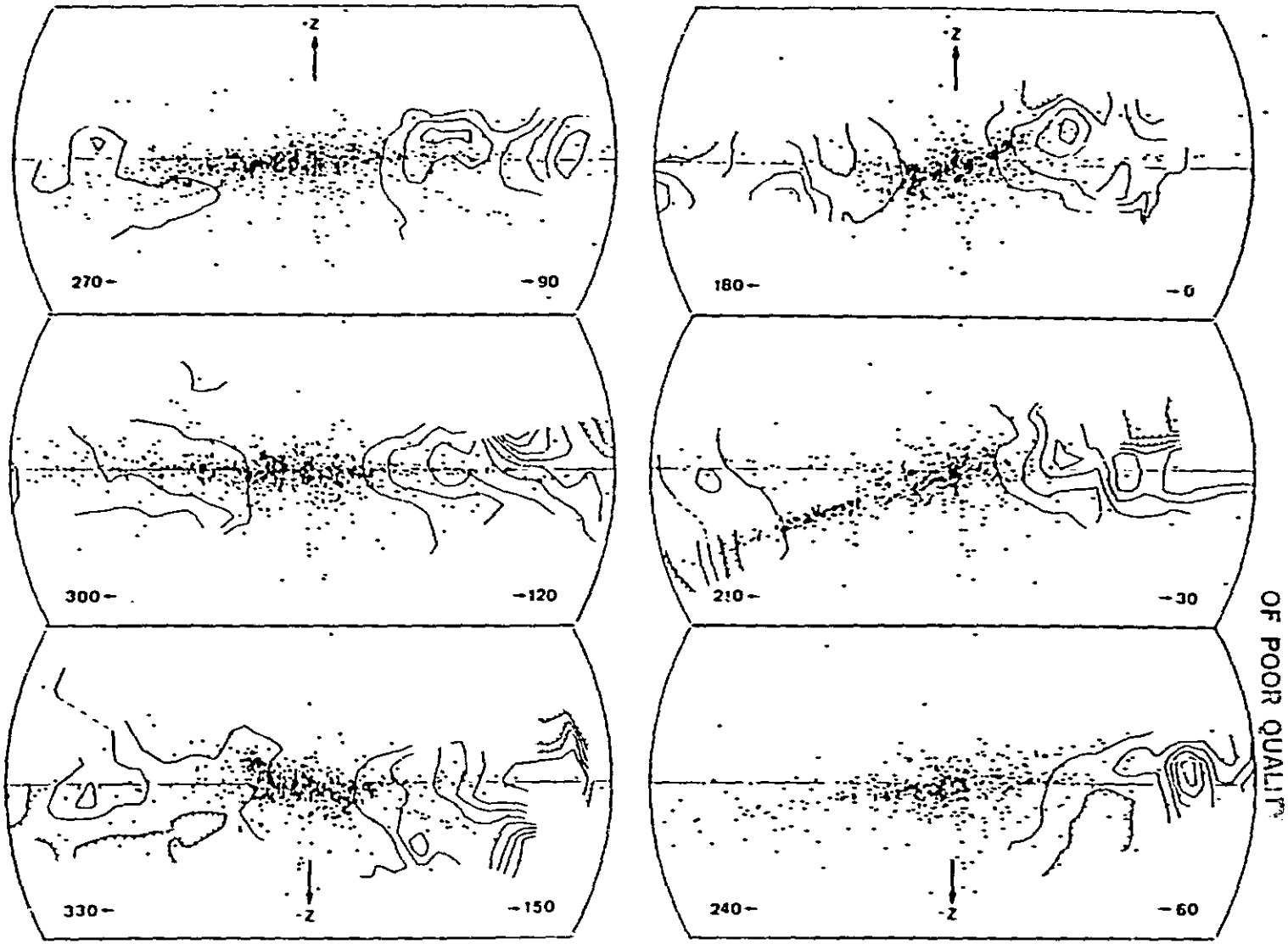

Color excess distribution in cross sections through the Galactic plane.

Figure 16.

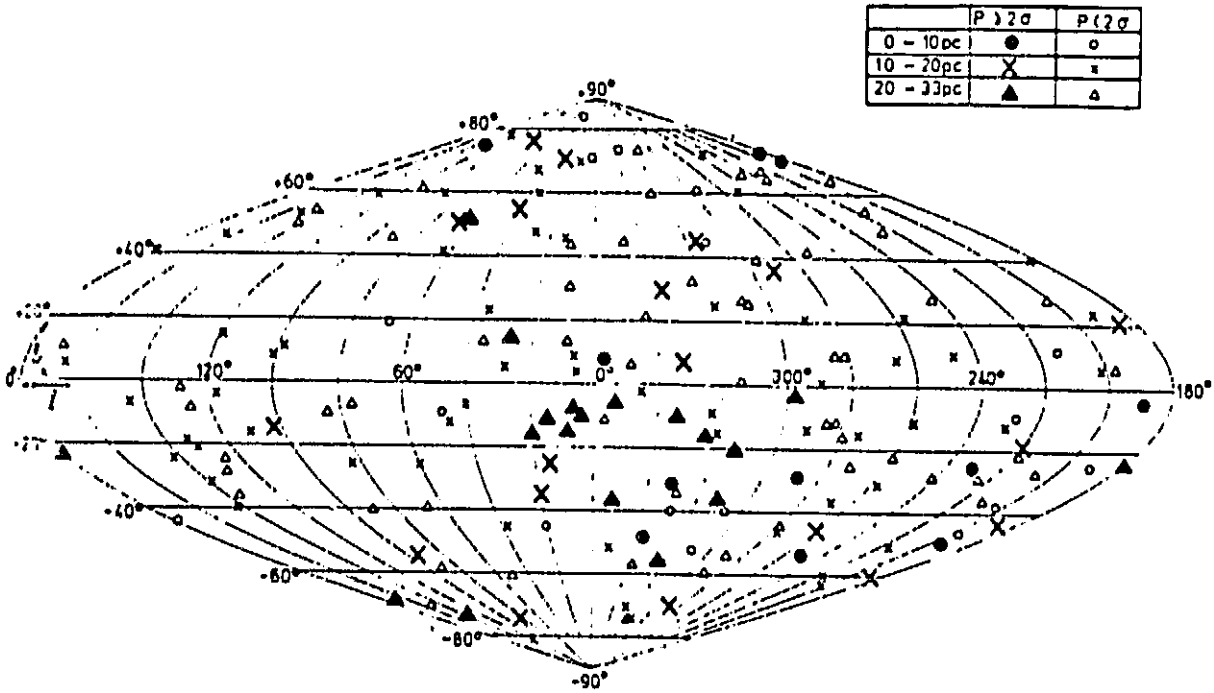

All-sky representation of the interstellar polarization for nearby stars. Large symbols denote degrees of polarization exceeding 4 in units of σ ($P > 2\sigma$, i.e. 95 %-confidence non-zero), small symbols polarizations less than this value. Rough distances are indicated by the choice of symbol. Data from Piirola (1977) included.

Figure 17.

8. Comprehensive Mission Success Criteria

A. Vehicle performance: Time above 200 km no less than 300 seconds.

B. Instrumentation:

1. Telemetry from PCM successfully recorded from T+55 to T+525 seconds.
2. All timed functions occur on schedule.
3. Uplink commands for pump power successful if necessary.

C. ACS

1. ACS and instrument remain co-aligned to within 1° during launch as verified by alignment checks before and after vibration tests at WFF and before flight at White Sands. Absolute position during flight must be confirmed by the experimenters on board star camera to be within 3° of the designated target direction.
2. Target direction will be acquired by T+90 seconds, and held for 360 seconds.
3. Pointing drifts less than .25° from the acquired direction as confirmed by the star camera.
4. Scan reaches a zenith angle of 90° before T+500 seconds.

D. Vacuum sealed section remains at a pressure less than 10^{-2} torr from the time it is sealed off at T-15 minutes until T+530 seconds as confirmed by the pressure sensor and the integrity of the thin filters.

E. Detector housings remain at a pressure less than 10^{-5} torr throughout the flight as confirmed by the pump currents and detector performances.

F. The thin filters that separate the detector housings from the vacuum sealed section must remain pinhole free and intact.

G. Experiment section recovered within 48 hours of flight.

9. Minimum Success Criteria

A. Vehicle performance: Time above 200 km no less than 200 seconds.

B. Instrumentation:

1. Telemetry from PCM successfully recorded for one of the two detectors for 100 seconds above 150 km.
2. Enough of the timed functions occur close enough to schedule to record 100 seconds of data from one of the detectors while above 150 km.

C. ACS

1. Primary target direction must be within 5° as confirmed by the experimenters on board star camera.
2. The primary target direction must be held for at least 100 seconds above 150 km. One of the detectors must be functioning during this interval.
3. The pointing must not drift more than .5° as confirmed by the experimenters on board star camera.

D. At least one of the detector housings must remain at a pressure less than 10^{-6} torr for at least 100 seconds during which the vehicle is above 150 km, and the ACS, telemetry, and timed functions allow data to be recorded from that detector.

E. At least one of the three thin filters must remain pinhole free and intact for at least 100 seconds during which the pressure in the detector chamber below the filter remains below 10^{-6} torr while the vehicle is above 150 km, the ACS, telemetry, and timed functions allow data to be recorded from that detector.

10. Support Requirements

Requested at WFF during integration:

A. Supply of dry nitrogen (99.9% purity minimum) for back filling the payload as necessary. One cylinder should be sufficient.

B. Availability of 208V 3 phase power for pumping system.

Requested at WSMR:

A. Supply of dry nitrogen (99.9% purity minimum) for back filling the payload as necessary. One cylinder should be sufficient.

B. Availability of 208V 3 phase power for pumping system at all locations the instrument will be tested, and on the tower.

C. Photographic coverage of horizontal checks, pre-flight launch tower operations (assembly etc.), launch and recovery.

D. At least 22 channels of real time data recorded on strip-charts during horizontal integration, pre-flight checks, countdown and during flight.

E. Monitoring of critical quantities through TM link during countdown, and at several pre-determined times before launch.

F. Communications link between tower and blockhouse.

G. Two two-axis oscilloscopes with video camera to record live flight time display. Two scalers for live display of countrates.

H. Two of the experimenters, Simon Labov and one other to accompany recovery crew to evaluate payload condition.

11. Special Analysis

No special analysis is required.

12. Payload Qualification and Status

Item	History	Tests	Comments
A. Mirrors	New	Vibration Thermal/Vacuum	at NARC at UCB
B. Gratings	New	Vibration Thermal/Vacuum	at NARC at UCB

C. Detectors	New	Vibration Thermal/Vacuum	at NARC at UCB
D. Collimators	New	Vibration Thermal/Vacuum	at NARC at UCB
E. Optical Bench Structure	New Thermal/Vacuum	Vibration at UCB	at NARC
F. Detector power supplies	Some new, some flew on 24.015	Vibration Thermal/Vacuum	at NARC at UCB
G. Pump power supplies	Some new, some flew on 24.015	Vibration Thermal/Vacuum	at NARC at UCB
H. Pumps	New	Vibration Thermal/Vacuum	at NARC at UCB
I. Pressure sensor	Flew on 24.015	Vibration Thermal/Vacuum	at NARC at UCB
J. Electronics	Some new, some flew on 24.015	Vibration Thermal/Vacuum	at NARC at UCB

Note: All vibration tests are done to levels for "New Design Payload, Vehicle Level Two" dated June 9, 1983

13. Redundant Systems

A. Both detectors have redundant high voltage supplies.

B. Pumps and pressure sensor all have redundant high voltage supplies.

C. Power lines are redundantly wired, with redundant timers.

14. Item History

A. Pressure sensor was flown on 27.026, 24.004 and 24.015.

B. Pressure sensor power supplies were flown on 27.026, 24.004 and 24.015.

C. Two of four detector power supplies were flown on 27.026, 24.004 and 24.015.

D. Low voltage power supplies were flown on 24.004 and 24.015.

E. Two of the four pump power supplies were flown on 24.004 and 24.015.

F. The interface electronics were flown on 24.004 and 24.015.

G. The detector electronics (charge amps and PPA's) are all new.

H. The camera controller is new.

I. The star camera may have flown on a previous sounding rocket.

J. The mirrors are new.

K. The gratings are new.

L. The collimators are new.

M. The detectors are new.

N. The optical bench structure is new.

15. Malfunctions

No malfunctions presently exist.

16. Discrepancies

No discrepancies presently exist.

17. Suspect Items

No suspect items presently exist.

18. Experimenter Master Check-off List

Principal Investigator: Stuart Bowyer

Project Scientist: Simon Labov

Integration support: Simon Labov

Electronics: Rick Raffanti

White Sands Operations: Simon Labov, Stuart Bowyer, Rick Raffanti

Recovery: Simon Labov, Unknown Experimenter

10. Experimenter Go/No-Go Launch Criteria

A. Pre-launch horizontal fully satisfactory

B. Tower checks fully satisfactory

C. Launch time within launch window

D. At T-3 hours, T-5 minutes and at other intermediate times when requested, the following must be monitored for go/no-go decision:

1. Filter integrity: this is monitored by running the on board ion pumps and pressure sensor and checking the pressure differential between the vacuum sealed section and the detector chambers.
2. Ion pump currents
3. Detector currents
4. Pulse height distributions
5. Live time oscilloscope display of detector images. Background rate and uniformity must be normal.

Red tag items:

A. Remove external high voltage power supplies.

B. Close detector isolation valves and secure.

C. Close port isolation valve and secure.

D. Disconnect and remove turbo pump from pump out port.

E. Close port access and electronics access doors.

20. Special Requirements in Event of a Scrubbed Mission

If scrub is due to range factors, payload can remain in tower indefinitely. In this case, the following are required.

A. An experimenter must enter the tower and reconnect the turbo pump and adjust valves accordingly. Once payload is pumped out again, the count may begin from T-15 minutes or earlier.

B. Rain protection

C. Periodic availability of TM link for instrument checkout.

21. Post Flight Requirements

A. Rapid recovery of payload.

B. Disassembly of major components of recovered payload.

C. WFF to prepare standard format 9 track digital data tapes.

Appendix B Telemetry Format

Data	Channel	Sample Rate
Data Detector 1, MSB's (X positions)	2-0-0	
Data Detector 1, MSB's (X positions)	6-0-0	3750
Data Detector 1, MSB's (X positions)	10-0-0	
Data Detector 1, LSB's (Y positions)	3-0-0	
Data Detector 1, LSB's (Y positions)	7-0-0	3750
Data Detector 1, LSB's (Y positions)	11-0-0	
Data Detector 2, MSB's (X positions)	4-0-0	
Data Detector 2, MSB's (X positions)	8-0-0	3750
Data Detector 2, MSB's (X positions)	12-0-0	
Data Detector 2, LSB's (Y positions)	5-0-0	
Data Detector 2, LSB's (Y positions)	9-0-0	3750
Data Detector 2, LSB's (Y positions)	13-0-0	
ACS Monitors	14-all	
Experiment Monitors:		
Pulse Height 1	15-0-3	156
Pulse Height 2	15-1-3	156
Countrate 1	15-2-5	39
I Mon 1	15-3-5	39
HV 1	15-4-5	39
Threshold 1	15-5-5	39
Deadtime 1	15-6-5	39
Pump 1A HV	16-7-5	39
Countrate 2	15-10-5	39
I Mon 2	15-11-5	39
HV 2	15-11-5	39
Threshold 2	15-13-5	39
Deadtime 2	15-14-5	39
Pump 2A HV	15-15-5	39
Pump 1A Current	15-18-5	39
Pump 1B Current	15-19-5	39
Pump 2A Current	15-20-5	39
Pump 2B Current	15-21-5	39
Pump 1B HV	15-22-5	39
Pump 2B HV	15-23-5	39
Door position bilevel	15-26-5	39
Door position analog	15-27-5	39
Sensor HV	15-28-5	39
Sensor Current	15-29-5	39
Temperature	15-30-5	39
Camera bilevel	15-31-5	39